



Contents lists available at ScienceDirect

Engineering Science and Technology, an International Journal

journal homepage: www.elsevier.com/locate/jestch



Potential use of graphene oxide as an engine oil additive for energy savings in a diesel engine

Özer Can ^{a,*}, Özgür Çetin ^{a,b}

^a Pamukkale University, Faculty of Technology, Automotive Engineering Department, Denizli, Turkey

^b National Defense University, Turkish Land Forces NCO Vocational College, Automotive Division, Balıkesir, Turkey



ARTICLE INFO

Keywords:

Graphene Oxide (GO)
Internal Combustion Engines
Engine Oil Additives
Nanoparticles
Engine Performance
Tribology

ABSTRACT

This study investigates the effects of graphene oxide (GO) nanosheets as an engine oil additive in fully synthetic SAE 10W-40 engine oil. GO concentrations in 0.5, 1.0, 1.5, and 2.0 mg/mL were added. The viscosity index (VI) increased by up to 7 % and thermal conductivity by 4–15 %. Tribological tests with a ball-on-disc mechanism showed that 1.5 mg/mL GO nanosheets additive gave the best results in reducing the coefficient of friction (COF) by 17 % and the total wear mass loss by 44 % on average. Based on the engine friction tests on the dynamometer, GO nanosheets reduced motored torque by up to 6 %, which represents the engine frictional losses, and improved mechanical efficiency by up to 2.8 % at certain engine speeds. An average improvement of 2.6 % in brake-specific fuel consumption (*bsfc*) and 2.7 % in brake thermal efficiency (*bte*) was observed across all engine speeds. The results of detailed engine tests suggest that the GO nanosheets additive has the potential to enhance the mechanical efficiency of internal combustion engines, leading to energy and fuel savings and indirectly contributing to reducing CO₂ emissions.

1. Introduction

Transportation activities consume a significant amount of energy worldwide, with a considerable portion used to overcome friction in mechanical systems [1–3]. In particular, internal combustion engines, experience energy losses due to friction and wear between moving parts, which can account for up to 17–20 % of their indicated power output [4–7]. To minimize friction and wear in internal combustion engines, various engine oils with different properties are used. The oil forms a lubricating film between moving parts, reducing friction and wear caused by the contact between the engine components [8,9]. However, due to various severe engine operating conditions, base engine lubricating oils derived from mineral or synthetic hydrocarbon blends are being further developed to also serve multiple purposes beyond their primary role of reducing friction and wear. The engine lubricating oils must also provide additional functions such as sealing between engine components, cleaning engine parts from soot, sediment and oil degradation compounds, protecting engine component surfaces from rust and chemical corrosion, buffering against contaminants, suspending waste material, and preventing deposition on the engine components [8–13]. Therefore, only using base engine oils cannot optimally meet all the

above-mentioned requirements. Additive packages containing organic or inorganic compounds in a wide spectrum such as friction modifiers (FM), anti-wear agents (AW), viscosity improvers, antioxidants, detergents and dispersants are added to the base engine oil. Thus, the performance of engine oils in various operating conditions largely depends on the properties of these additives and the formulations of the additive packages [8–12,14,15]. Advancements in internal combustion engine technology such as higher compression ratios, downsizing with super or turbocharging, increased engine speeds, start-stop systems, exhaust after-treatment systems etc. demand more properties from engine lubricating oils [16,17]. As a result, base engine oils containing these additives face challenges in providing the necessary friction and anti-wear properties under the high combustion pressure and temperature conditions associated with these developments. Furthermore, the use of some conventional additives such as zinc dialkyl-dithiophosphates (ZDDP) or the limitation of the sulfur and phosphorus contents raises environmental concerns due to toxic exhaust emissions and particulate matter formation [4,17–19]. This has also led to a growing interest in environmentally friendly additives known as new-generation green additives, which are non-toxic or low-toxic, biodegradable, and compatible with engine exhaust after-treatment systems [20].

* Corresponding author.

E-mail address: ozercan@pau.edu.tr (Ö. Can).

Consequently, the use of engine oil additives has become a critical area of research and development in the automotive industry, aiming to improve the efficiency, durability, and reliability of internal combustion engines [21–26].

The impact of multi-grade and low-viscosity engine oils on fuel efficiency improvements and engine reliability has been extensively studied. The results indicate that reducing engine oil viscosity effectively enhances fuel efficiency, although it raises concerns about engine durability, particularly under high-temperature and high-speed operating conditions [24,27–29]. Due to the growing need to reduce fuel consumption and CO₂ exhaust emissions, the usage of new engine oil additives to reduce friction can provide up to 10 % improvement in mechanical efficiency and a 1–2 % decrease in fuel consumption in existing engines [22]. In this quest, the use of nanoparticles as lubricating oil additives has been widely investigated due to their unique properties. Nanoparticles have different shapes and structures, much smaller sizes, and higher specific surface areas compared to conventional additive components [30,31]. Therefore, their excellent thermal and lubrication properties make nanoparticles a promising choice as lubricant additives. In recent years, various nanoparticle additives have been investigated in the literature, which can be roughly divided into mainly four groups such as metals, metal oxides, carbon-based materials and boron-based materials. As an example of these, various nano metal additives like Fe, Cu, Sn and CO; different nano metal oxide additives such as TiO₂, CUO, ZnO, Al₂O₃ and ZnAl₂O₄; various carbon-based materials including fullerene, carbon-nanotubes, graphene, graphene oxide (GO); and boron-based nano additives such as boric acid, hexagonal boron nitride, zinc borate, cerium borate, which can be found in the literature [14,32–35]. These studies primarily focused on investigating tribological properties and friction reduction mechanisms, while some of these also concentrated on the synthesis and preparation of particles on the nanoscale. In general, most of studies consistently showed that the addition of nanoparticles to base oils enhances the coefficient of friction (COF) and anti-wear properties, while also improving viscosity and thermal conductivity. The friction reduction and anti-wear effects of nanoparticles in the base engine oil are explained by various mechanisms that can occur alone or in combination, such as interlayer sliding, tribofilm deposition and repair effects e.g [14,15,30,32,36,37]. Additionally, these studies also indicated that the tribological characteristics of the lubricating oils are influenced by various factors, such as the composition, shape, concentration, size, and dispersion stabilization of the nanoparticles within the base engine oils [14,31,34,38]. However, most of these studies in the literature remained in the friction bench testing phase, and the experiments on internal combustion engines were also very limited.

Sarma et al. [39] investigated the effects of Cu and TiO₂ nanoparticle additives on the performance of a four-stroke gasoline engine powered two-wheeler on a motorcycle chassis dynamometer. They observed a 4–7 % improvement in *bte* depending on the reduction in engine frictional power. Sgroi et al. [19] conducted engine and vehicle chassis dynamometer tests to investigate the usage of MoS₂ nanoparticles as an anti-friction and anti-wear additive to a fully formulated engine oil. They observed a reduction of up to 5 % in fuel consumption under certain engine operating points in the engine dynamometer measurements, while the average fuel savings was observed at 1 % on the New European Driving Cycle (NEDC) on the chassis dynamometer. They also found that MoS₂ nanoparticles were fully compatible with existing passenger vehicles' after-treatment systems. Ali et al. [4] performed engine dynamometer tests by using Al₂O₃/TiO₂ hybrid nanoparticle additives to improve the performance of gasoline engines at all operating points and the NEDC driving cycle. Their results indicated that using Al₂O₃/TiO₂ hybrid nanoparticles reduced total engine frictional power losses by 5–7 % and improved engine mechanical efficiency by 1.7–2.5 %, which resulted in increases in engine *P_e* and torque. The fuel consumption savings they achieved during the NEDC tests were equivalent to a fuel economy of around 4 L/100 km in the urban phase. Also,

they reported that Al₂O₃/TiO₂ nanoparticles accelerated the engine warm-up phase by 24 %. Ali et al. [5] investigated the tribological behavior using graphene (Gr) nanoparticles for energy saving and reducing exhaust emissions in a gasoline engine. In their engine dynamometer test results, Gr nanoparticles added to SAE 5W-30 engine oil increased *P_e* and torque in the 7–10 % range due to a 6 % reduction in total engine frictional power. Also, they reported a 17 % reduction in cumulative fuel mass consumption with road load simulation during the NEDC test. Koita et al. [38] investigated the effects of Al₂O₃ or SiO₂ nanoparticles additions into SAE 15W-40 engine oil for the performance of a four-stroke diesel engine. They reported that the addition of Al₂O₃ in 0.3 wt% minimized *bsfc* and provided maximum *bte* at various engine loads. Singh et al. [40] synthesized nanographite and spherical carbon nanoparticles as two types of new carbon nanostructures with graphite structural units. They conducted engine performance tests with nano graphite-based additives due to better results in tribology tests. In their engine performance results, engine *bsfc* values were reduced by up to 18 % and *bte* by up to 22 %. Singh et al. [6] investigated the effect of graphene nano-platelets additions to SAE 15W-40 engine oil on fuel consumption and piston ring wear in the gasoline engine. In their results, graphene nano-platelets were found to contribute to an increase in *M_e*, while simultaneously reducing *bsfc* by 5.3 %–6.5 %. These improvements were attributed to an improvement in engine mechanical efficiency by 1.7 %–3.46 %. Hetri et al. [7] used coconut oil as a base oil and added the 2D nanocomposite Al₂O₃/Gr additives to base lubricating oil. They conducted tribology tests in linear reciprocating tribometer and engine performance tests with engine dynamometer, and compared results with SAE 15W-40 engine oil. Their results showed a 28 % reduction in COF in tribology tests and an 8 % reduction in *bsfc* with lower CO, SO₂ and NO_x emissions in engine tests. In another study, Lue et al. [41] investigated nano-SiO₂ particles as an engine oil additive in 4-stroke single-cylinder scooter engine. They performed engine tests with the ECE-40 driving cycle test on the four-quadrant motorcycle chassis dynamometer. In their results, fuel consumption decreased by 15.22 % on average and acceleration performance increased by 10.3 % with lower exhaust emissions.

Frictional losses in an engine result from various sources, such as hydrodynamic friction in the crankshaft and camshaft journal bearings, mixed or boundary lubrication friction in the piston ring pack, and valve train [8,9,42,43]. Therefore, the measurement of overall frictional losses and engine mechanical efficiency on the engine dynamometer holds significant importance due to the different lubrication regimes that occurred on the component base through the engine speed. It is also important to develop the relationship between the friction and wear performance results of friction bench and engine dynamometer tests. As seen from the literature, there are a limited number of studies on nanoparticle engine oil additives that investigate both tribological friction bench test results and engine performance test results on a dynamometer under real operating conditions.

In addition to the previously mentioned nanoparticle additives, carbon nanomaterials have recently gained significant attention. Among them, Gr and GO, as two-dimensional materials, stand out for their notable characteristics, including high specific surface area, excellent mechanical strength with high load-bearing capacity, higher thermal conductivity, low surface energy, high chemical stability, and robust intramolecular bonds while maintaining weak intermolecular bonds [32,36,37,44–48]. GO can provide excellent anti-wear and anti-friction properties to the lubricating oil. However, to ensure the effective use of GO as an additive, it is necessary to modify the surface of the GO nanosheets to prevent their agglomeration and enhance their solubility in the base oil. Therefore, more research is needed on this topic to provide more information on the effects of GO nanosheets as an engine oil additive on engine performance. To meet this gap, this study investigates the effects of GO nanosheets as an engine oil additive in fully synthetic SAE 10W-40 base engine oil. Four different concentrations of GO (0.5, 1.0, 1.5, and 2.0 mg/mL) were added to the base engine oil.

Tribological performance tests with Ball-on-Disc tribometer test device were conducted initially to evaluate different lubrication regimes on the Stribeck curve, including boundary, mixed and hydrodynamic lubrication conditions. Then, the concentration ratio that provided the best results in the tribological bench tests was tested on the engine dynamometer. Thus, the potential of GO nanosheet addition to improve engine mechanical efficiency, saving energy and fuel, and consequently decrease CO₂ emissions were examined.

2. Material and methods

2.1. Characterization properties of graphene oxide nanosheets

In this study, nano-sized 2D GO sheets with 2–5 layered structures (Product code: NG01GO0102) were obtained from Nanografi Nano Technology Co. Ltd. in Ankara/Turkey. The characterization analysis results of the GO nanosheets provided by the production firm are presented in Fig. 1. According to CHNSO elemental analysis by using Leco, CHNS-932 model device, the chemical composition of the GO nanosheets is as follows: C (52.61 % wt%), O (46.94 wt%), and others (0.45 wt%). High Resolution Scanning Electron Microscope (SEM) images obtained by using the QUANTA 400F model device are shown in Fig. 1-A. Transmission Electron Microscope (TEM) images obtained by using Hitachi HighTech HT7700 model device are shown in Fig. 1-B. As it is seen from the images, the dimensions of the GO nanosheets supplied by the company are approximately 500–700 nm. Also, the GO nanosheets have a plate-like shape with non-sharp edges, and some areas on the surface have folded and wrinkled corners. Furthermore, there are no residues that may be causing any roughness or pollution on the surfaces of the sheets. The TEM image also confirms that the GO nanosheets have been exfoliated and have layered structures. The X-ray diffraction pattern obtained by using Rigaku Ultima-IV for the GO nanosheets in the 2θ range of 5°–40° is seen in Fig. 1-C. The first strongest diffraction peak position is seen at approximately 10° and the second broad peak with less intensity is seen around 24°. According to the literature, the first peak position indexed to 002 at 10° is very characteristic for GO materials and it is reported to be roughly between 0.8 and 0.9 nm interlayer distance [13,49–52]. The second peak at about 24° is thought to be due to the impurity of Gr or the inspected sample not being completely dry [52]. As a result, the X-ray diffraction image of the GO nanosheets obtained from the firm shows good qualitative agreement with the literature.

2.2. Surface-Modification of graphene oxide Sheets, preparation of the Mixtures, and dispersion stabilities

In this study, to ensure solubility and prevent agglomeration of the GO nanosheets additives in the base engine oil, the surfaces of the GO nanosheets were modified by using pure oleic acid ($\geq 99\%$ (GC), Sigma-Aldrich, Product Code: O1008-5G), which is the most preferred surfactant. Since the oleic acid includes hydrophilic hydroxyl and alkyl groups, which are important for increasing the solubility and dispersion of nanoparticles in the oils, this process results in a change the characteristics [13,53–55]. A homogeneous slurry was prepared by adding 1.0 g of GO in 60 mL of 200-proof ethanol (Sigma-Aldrich, Product Code: E7023) in the ultrasonic bath. Then, 1.0 g of oleic acid was added to the homogeneous GO solution and mixed thoroughly for half an hour at room temperature. After extracting ethanol under reduced pressure, the material was washed several times with ultrapure deionized water. The resulting oleic acid-coated GO nanosheets were dried at 70 °C and stored in a vacuum desiccator. A fully synthetic SAE 10W-40 engine oil (Petrol Ofisi, Maximus LA 10 W-40) was used as the base engine oil, which is commercially available in Turkey. The mixtures were prepared by adding GO nanosheet additives at 4 different concentrations (0.5, 1.0, 1.5, and 2.0 mg/mL) into the base engine oil. GO nanosheet additives were weighed using a Shimadzu ATX 224 Unibloc analytical balance

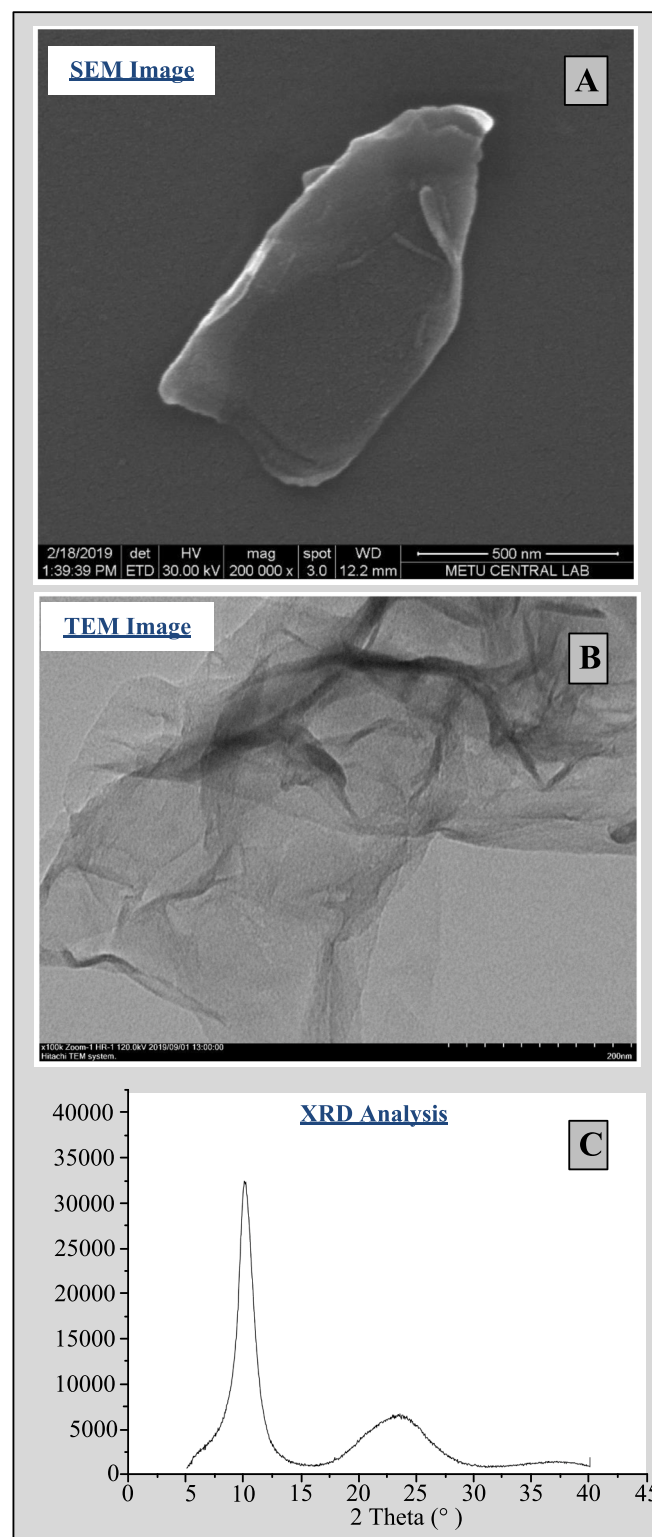


Fig. 1. SEM, TEM and XRD analysis results of the graphene oxide nanosheets.

with an accuracy of 0.1 mg, then dispersed homogeneously in the base engine oil using a Hielscher UP400S (400 W, 24 kHz) ultrasonic sonication probe for 1 h at 74 % amplitude and 1 cycle. This process ensured the formation of a uniform and stable suspension of the base engine oil with GO nanosheet additives. Also, the dispersion stability of the prepared mixtures was monitored for up to 30 days. As shown in Fig. 2, even after 30 days following the completion of the ultrasonic mixing

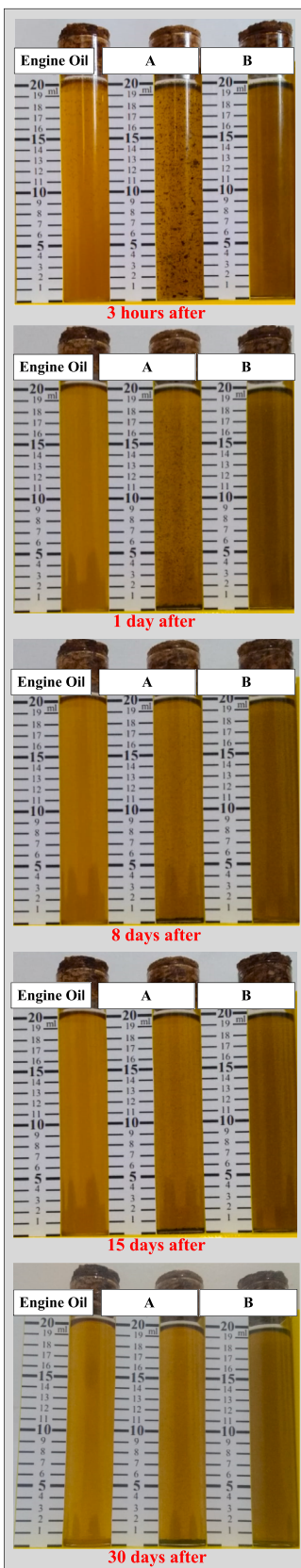


Fig. 2. Dispersion stability of the base engine oil (SAE 10W-40) with graphene oxide nanosheets additive in 1.5 mg/mL concentration (A: Mechanical mixing process and B: Ultrasonic mixing process).

process, a significant portion of GO nanosheet additives remained homogeneously dispersed. This result showed that the surface modification process was found to be beneficial in the stability of the mixture samples. Whereas, even on the first day after the mechanical mixing process, non-uniform dispersions of GO nanosheet additives caused by their agglomerations in the base engine oil were observed and most of them tended to settle to the bottom of the sample tube over time. Therefore, an ultrasonic mixing process is necessary to prevent the initial agglomeration of the nanoparticles within the engine oil.

2.3. Rheological measurements of prepared mixtures

The dynamic viscosities of the prepared samples were measured using an AND SV-10 model tuning-fork vibration type viscometer at different temperatures ranging from 0 to 100 °C. The densities of the samples at 40 and 100 °C were measured with a Rudolf Research Analytical DDM 2911 model density meter. Also, VI of the samples were calculated according to ASTM D2270 [56]. The thermal conductivities of the samples were also measured at different temperatures ranging from 20 to 100 °C with P.A. Hilton Limited-H471 model test apparatus, whose measuring method is based on the steady-state parallel method [57–60].

2.4. Tribological performance tests with a Ball-on-Disc mechanism

As seen in Fig. 3, tribological performance tests of the samples were performed according to ASTM G99-95a by using a Turkyus PODWT model Ball-on-Disc tribometer test device [61]. The configuration of the tribometer device consists of a rotating disc at constant speed against a stationary steel ball specimen under load, which was also immersed in engine oil. The rotating disc for the abrasive surface area was made from 100Cr6 steel material with a 165 mm diameter with 64 HRC surface hardness, and 0.8 Ra surface roughness. The stationary ball specimen had an 8 mm diameter and was made from AISI 420-B 45 with a 50 HRC surface hardness to be subjected to abrasion on the disc. For each test, the contact area of the ball specimen on the disc was completely immersed in a 30 mL prepared sample engine oil bath in a reservoir on the rotating disc at room temperature. In addition, to prevent engine oil starvation due to the effects of centrifugal forces at different rotational speeds, a flexible scraper was used on the disc track for the replenishment mechanism and uniform engine oil film formation. To assess different lubrication regimes, i.e., boundary, mixed, and hydrodynamic lubrication conditions, the tests were conducted at 13 different testing points covering the Stribeck curve. Viscosity change on Stribeck parameters was neglected in the experiments. The rotational speeds of the disc were swept from 8 to 155 rpm under loads of 20, 40, and 60 N (which corresponds to 1428.6, 1799.9 and 2060.4 Mpa initial Hertzian contact pressures, respectively) to the stationary ball specimen at a distance of 0.07 m from the center of the disc. The normal force (P) was applied vertically to the ball specimen using a death-weight lever mechanism. The friction force (F) at the contact area was also measured using a strain-gauge type load cell. The measurements were recorded by taking 25 data points per second for 5 min for each sample at test points. The dynamic COF (μ) between the ball specimen and the disc was calculated from Equation (1). An average COF (μ) was also calculated for every test point.

$$\mu = \frac{F}{P} \quad (1)$$

Stribeck parameter (λ) was calculated with dynamic viscosity (η), the relative speed between contact surfaces (V) and load on the contact surface (F_n) as follows [62–64].

$$\lambda = \frac{\eta \cdot V}{F_n} \quad (2)$$

At the end of each test, the Wear Scar Diameters (WSD) on the ball

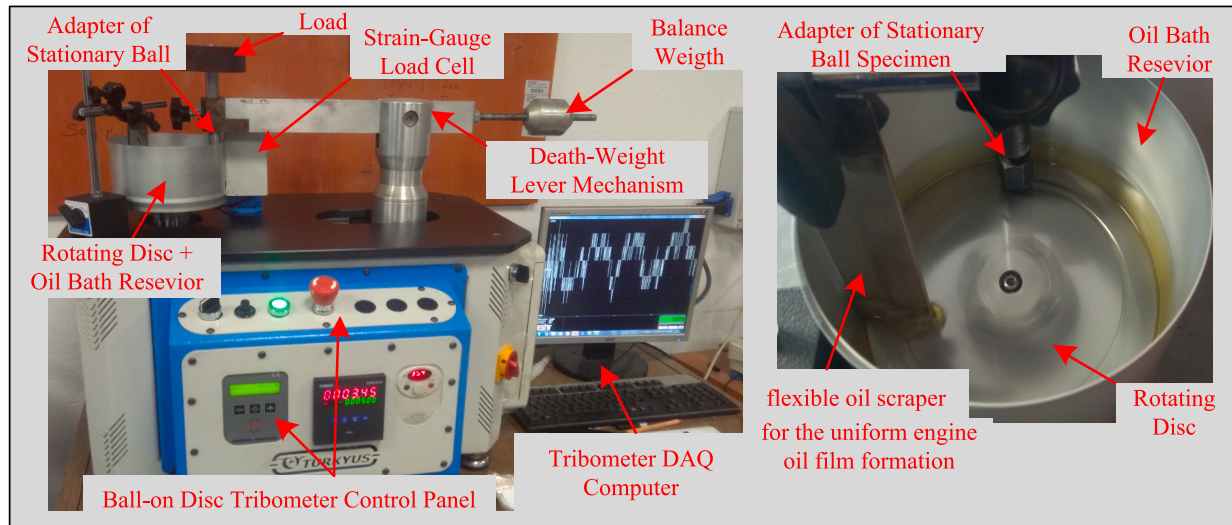


Fig. 3. General view of the Ball-on-Disc tribometer test device.

specimens were measured by using a Nikon Eclipse LV150NL optical microscope. Microstructures of the worn surfaces on some of the ball specimens were also investigated with SEM and Energy Dispersive X-ray Spectrometry (EDS) analysis by using a Zeiss Supra 40VP. As seen in Fig. 4 and with the following equations, the wear loss on the ball specimen was determined volumetrically with a simple geometric calculation from the measured WSD. The plastic deformation on the contact area was ignored, and the wear scar profile was assumed to be flat and circular [65–67]. The wear loss in mass was also found by multiplying this value with the density of the ball specimen.

$$V = \pi \left[h.R^2 - \frac{R^3}{3} + \frac{(R-h)^3}{3} \right] \quad (3)$$

$$h = R - \sqrt{R^2 - s^2} \quad (4)$$

2.5. Engine tests

The engine tests were conducted on a single-cylinder, natural-aspirated, air-cooled, four-stroke, DI diesel engine, which was coupled to the PCS brand engine test bed (Fig. 5). The technical specifications of the test engine are listed in Table 1. An ABB VH3.5 model active AC electric dynamometer with 16.7 kW power absorption capacity at 3000 rpm was driven by the ABB ACS800 unit and controlled by a dedicated NI

Labview-based PCS dynamometer automation and control program. The engine torque was measured from the shaft between the engine and the dynamometer using a non-contact Tilkom M40 model telemetry torque sensor with a capacity of 200 Nm and an accuracy of 0.1 %. The engine speed was measured with a 1024 pulse/revolution incremental encoder with an accuracy of ± 0.1 rpm, which was internally integrated into the AC dynamometer motor. The fuel consumption was measured with a Radwag WTC 200 high-precision electronic balance. The temperatures of fuel, intake air, engine oil and exhaust gas were measured with K-type thermocouples. The ambient pressure, temperature and humidity of the engine test room were measured with the PCS85 meteorological transmitter. All of the measurements were collected and recorded instantly with a NI data acquisition system in 19" rack-mounting, which was integrated into the dynamometer automation and control program.

To evaluate the frictional losses on the test engine, it was operated under steady-state conditions in both motoring and firing modes at full engine load. The tests were performed at five different engine speeds ranging between 1700 and 2800 rpm and seven different engine crankcase oil temperatures between 40 and 100 °C. To precisely simulate the firing engine conditions, motored engine tests were performed with fuel injections cut-off immediately after firing engine tests. Also, in this study, since the test engine was operated un-throttled at different constant engine speeds, the engine friction losses (pumping + friction losses) were assumed to be mostly dependent on the engine speed [5,8,9,42,68]. In the fired engine tests, effective engine brake power (P_e) in kW can be calculated with measured brake engine torque (M_e) (i.e., fired engine torque) in Nm and engine speed (n) in rpm.

$$P_e = \frac{M_e \cdot n}{9549} \quad (5)$$

Also, the engine mean effective pressure ($bmeep$) in bar can be calculated with (P_e) in kW, engine displacement volume (V_d) liter and the number of cycles per engine crankshaft revolution (f).

$$bmeep = P_e \cdot \frac{V_d}{10^3} \cdot \frac{n}{60 \cdot f} \quad (6)$$

The engine frictional power (P_f) in kW was calculated with measured motored engine torque (M_m) in Nm.

$$P_f = \frac{M_m \cdot n}{9549} \quad (7)$$

The mean engine frictional pressure ($fmeep$) in bar can be calculated with (P_f).

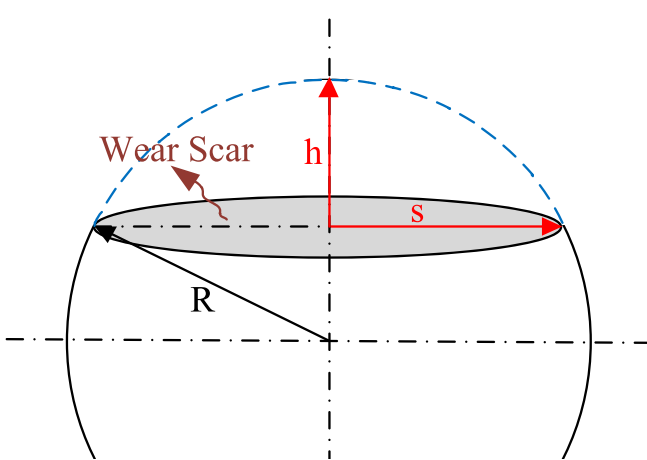


Fig. 4. Schematic view of ball specimen with a worn surface.

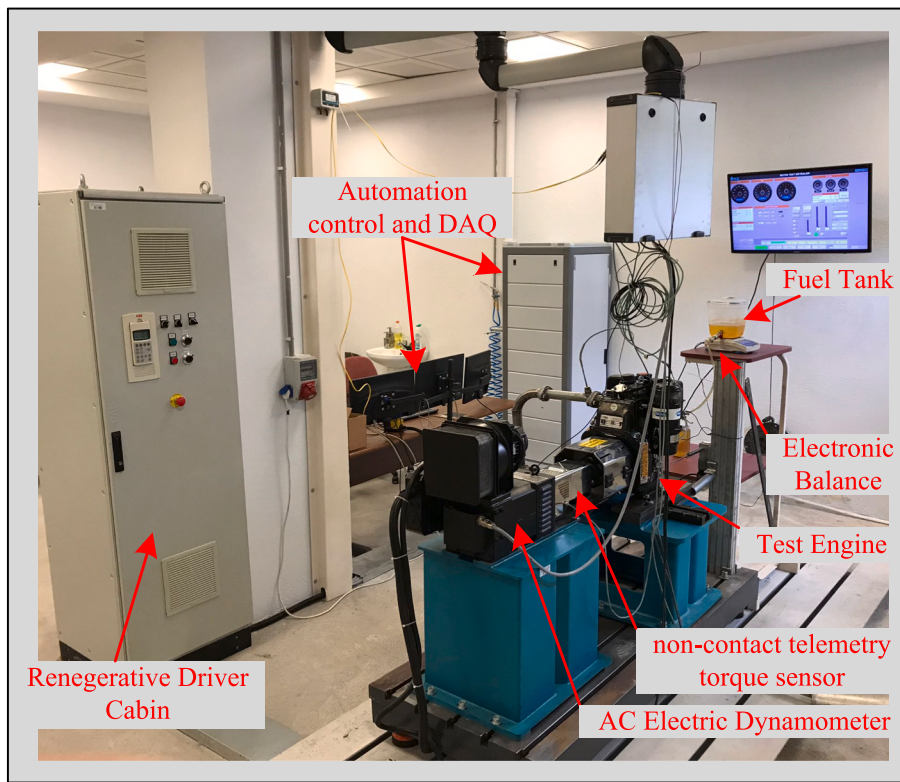


Fig. 5. General view of the Engine test bed.

Table 1
Specifications of the test engine.

Make/Model	Antor/6LD400
Engine type	DI-Diesel
Aspiration	Natural aspirated
Cooling type	Air cooled
Cylinder number	1
Bore x stroke (mm)	86x68
Displacement volume (cm ³)	395
Compression ratio	18:1
Maximum power (kW)	5.4@3000 rpm
Maximum torque (Nm)	19.6@2200 rpm

$$f_{mep} = P_f \cdot \frac{V_d}{10^3} \cdot \frac{n}{60} \cdot f \quad (8)$$

(f_{mep}) is also a difference between the net indicated mean effective pressure (n_{mep}) and brake mean effective pressure (b_{mep}).

$$f_{mep} = b_{mep} - n_{mep} \quad (9)$$

The engine mechanical efficiency (η_m) can be calculated with the following equation.

$$\eta_m = \frac{b_{mep}}{n_{mep}} = \frac{b_{mep}}{b_{mep} - f_{mep}} \quad (10)$$

The engine brake specific fuel consumption ($bsfc$) in g/kWh can be calculated with the fuel flow rate (\dot{m}_f) in g/h and (P_e).

$$bsfc = \frac{\dot{m}_f}{P_e} \quad (11)$$

The engine brake thermal efficiency (bte - η_t) was calculated with ($bsfc$) and fuel heating value (Q_{HV}) in MJ/kg.

$$\eta_t = \frac{3600}{bsfc \cdot Q_{HV}} \quad (12)$$

Measurements were repeated three times under steady-state conditions and averaged values were used. All of the measurement accuracies and uncertainties in the derived values were less than 0.3 %.

3. Results and discussion

3.1. Viscosity results

Fig. 6 shows the variations in the dynamic viscosities of the base engine oil with different concentrations of GO nanosheets additive at temperatures ranging from 0 to 100 °C. As generally expected, all samples exhibit a logarithmic decrease in viscosity with increasing temperature and show Newtonian behavior in the temperature range.

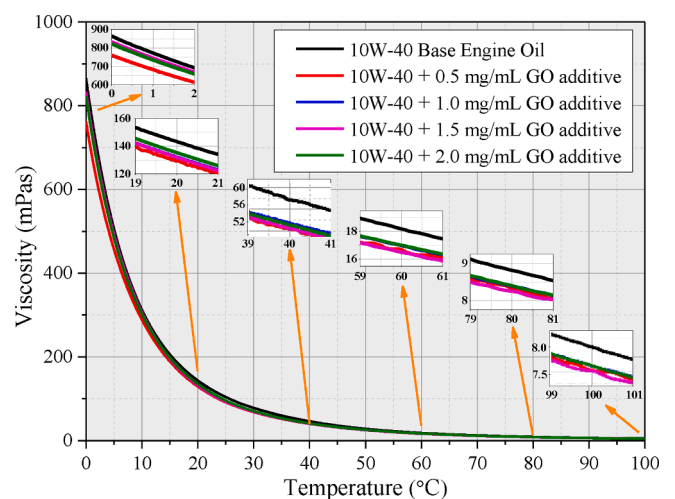


Fig. 6. Variation of dynamic viscosities of base engine oil with GO nanosheet additives depending on temperature.

The addition of GO nanosheet additives into the base engine oil also showed similar rheologic behavior on the viscosity. However, the dynamic viscosities of the base engine oil decreased with the addition of the GO nanosheets additive at all concentrations in the temperature range between 0 and 100 °C. The dynamic viscosity values decreased in the range of 2–14 % with the GO nanosheets additive, particularly at temperatures above 40 °C. These changes in viscosity can be explained by the settling of multi-layered GO nanosheets between adjacent engine oil layers, which provides relative ease of movement between the oil layers and thus reduce viscosity as a result of the reduction in shear stress [44,69–71]. On the other hand, the viscosity values slightly increased and approached the base engine oil values as the concentration of GO nanosheets additive increased at low temperatures around 0 °C. In this case, the nanoparticles tend to agglomerate and form larger, asymmetrical particles as the GO concentration increases, which slightly prevents the relative movement of adjacent oil layers over each other [38,45,72]. Thus, a slight increase in viscosity was observed, especially at low temperatures and high GO concentrations. However, when comparing GO added base engine oils among themselves, there was a negligible change in the dynamic viscosities at temperatures of 20 °C and above due to the increase in GO concentrations. The variation of this trend in viscosity at higher temperatures was probably attributed to the weakening of attractive intermolecular interactions in suspended GO nanosheets with increasing temperature [38,70,73].

VI of the samples shown in Table 2 were calculated according to the ASTM-D2270 standard using kinematic viscosities at 40 °C and 100 °C. As seen from the results, the VI values of the samples showed a slight increase up to 7 % with the addition of GO nanosheet additives at different concentrations when compared to the base engine oil. This increase in VI indicates that the base engine oil with GO nanosheet additives can operate successfully over a wide temperature range without changing the viscosity too much [74,75]. Low viscosity and high VI have a significant impact on the fuel economy by reducing frictional losses through the shear-thinning tendency of the oil films at the high shear rates present in engine components (piston rings and main crankshaft journal bearings). [28,36,71,76,77]. Also, the GO nanosheet additives can be considered as an alternative VI improver because they have sufficient shear stability due to their inter-sheet shearing ability and high load-carrying capacity [71]. Thus, they do not degrade easily and lose their effectiveness during severe engine running conditions compared to polymer type VI improvers [78].

3.2. Thermal conductivity results

Fig. 7 shows the variations in the thermal conductivity coefficients of the base engine oil with different GO nanosheets additive concentrations at temperatures from 20 to 100 °C. As illustrated in Fig. 7-A, the thermal conductivity of all prepared samples increased almost linearly with an increase in temperature. Furthermore, Fig. 7-B shows that the thermal conductivity increased with the increasing concentration of GO nanosheets additive at each temperature. The thermal conductivity of the base engine oil increased in the range of 4–15 % with GO nanosheet

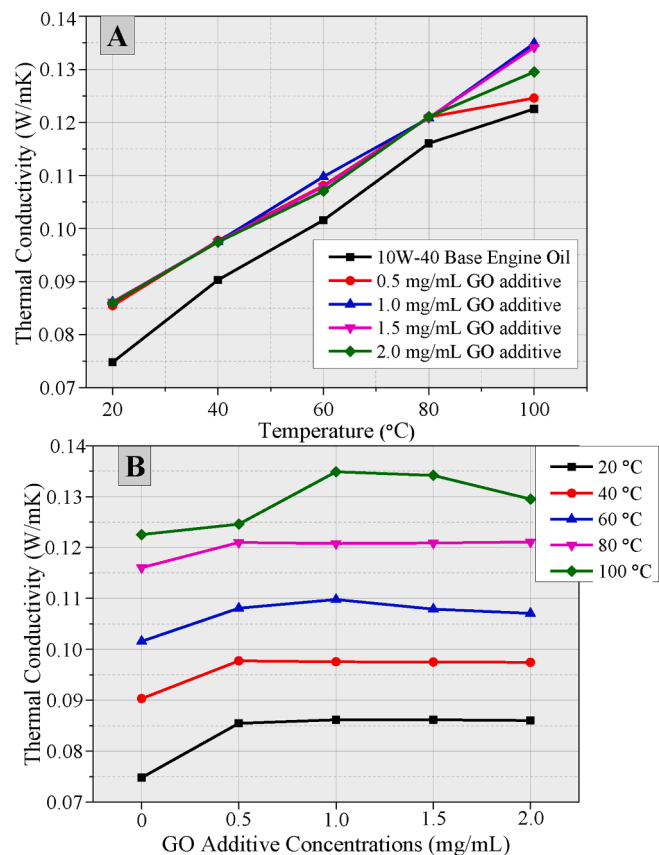


Fig. 7. Effect of GO concentrations on thermal conductivity of 10 W-40 base engine oil at different temperatures.

additives at all concentrations. The improvement in thermal conductivity can be explained by the high surface-to-volume ratio and the thermal conductivity properties of the GO nanosheets [72,73,75,79,80]. Another reason for this improvement can be attributed to the increase in Brownian motion of GO nanosheets with increasing temperature (random rotational and translational movements), resulting in nanoparticles moving and facilitating heat transport, thus improving thermal conductivity [70,73,80–82]. Moreover, it was agreed that the reduction in the viscosity also increased the Brownian motion of the particles. However, it can be speculated that the combination of the increasing Brownian effect at high temperatures and the increase in GO concentration may play a dominant role in the clustering effect due to the random movement of GO nanosheets in response to the high-frequency collisions of base engine oil molecules [70,81–85]. Nevertheless, the results at 100 °C indicate that the existence of such micro-scale aggregations of GO nanosheets limits the possibility of improving thermal conductivity. [83]. As a consequence, the enhanced thermal conductivity of the engine lubricating oils will be beneficial in the transfer of heat generated by friction and the thermal stability of the engines. It will also contribute to the accelerating of the engine's warm-up phase [4,75].

3.3. Coefficient of friction and wear results

The results of tribological performance tests are shown in Fig. 8, covering 13 different test points on the Stribeck curve to evaluate the different lubrication regimes including boundary, mixed, and hydrodynamic lubrication conditions. All the Stribeck curves obtained for all samples exhibited almost similar characteristic trends, with transitions between different lubrication regimes occurring at the same points for all samples. These observed results suggest an identical and uniform

Table 2
Viscosity indexes of base engine oil with GO nanosheet additives.

Base Engine Oil (SAE 10W-40)	GO nanosheet additive concentration			
	0.5 mg/ mL	1.0 mg/ mL	1.5 mg/ mL	2.0. mg/ mL
Viscosity @ 40 °C (mm ² / s)	58.80	51.35	52.59	51.59
Viscosity @ 100 °C (mm ² / s)	8.06	7.64	7.69	7.58
Viscosity Index (VI)	103.90	112.97	110.54	111.14
				110.37

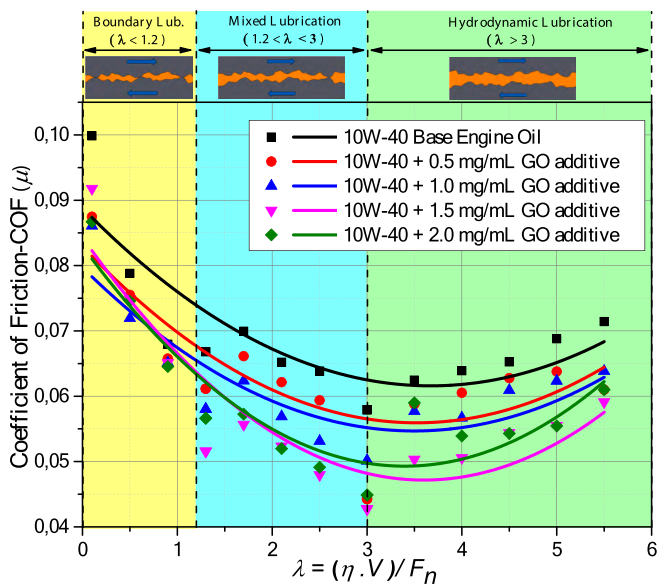


Fig. 8. Effect of GO concentrations on tribological performance test results.

friction-driven mechanism [64].

As can also be seen in the results, significantly lower COF was observed at all concentrations of added GO nanosheets in all lubrication regimes when compared to base engine oil. As also seen from Table 3, the obtained results for the boundary lubrication regime ($\lambda < 1.2$) showed that GO nanosheet additives in 0.5, 1, 1.5 and 2.0 mg/mL concentrations reduced the COFs by up to 12.4 %, 13.8 %, 8 % and 13.16 %, respectively. In the mixed lubrication regime ($1.2 < \lambda < 3$), GO nanosheet additives in 0.5, 1, 1.5 and 2.0 mg/mL concentrations reduced the COFs by up to 23.55 %, 16.77 %, 26.14 % and 23.04 %, respectively. In the hydrodynamic lubrication regime ($\lambda > 3$), GO nanosheet additives in 0.5, 1, 1.5 and 2.0 mg/mL concentrations reduced the COFs by up to 23.56 %, 13.42 %, 26.15 % and 22.5 %, respectively. In the boundary lubrication regime, the lowest COF was obtained with 1.0 mg/mL GO nanosheet concentration, while it was obtained with 1.5 mg/mL concentration for the mixed and hydrodynamic lubrication regimes. However, when the concentration was increased to 2.0 mg/mL, the COFs increased slightly in all lubrication regimes compared to the 1.5 mg/mL concentration, while remaining below the base engine oil values. After considering the dynamic conditions of the main engine friction components (main bearings, valve train, and piston rings), operating under different lubricating conditions and according to the obtained results, the best concentration amount was determined as 1.5 mg/mL with its tribological performance in the mixed lubrication regime [42,43]. This is also supported by the average values for all lubrication regimes given in Table 3, which show that 1.5 mg/mL concentration gives the lowest COF value. Fig. 9 also shows the

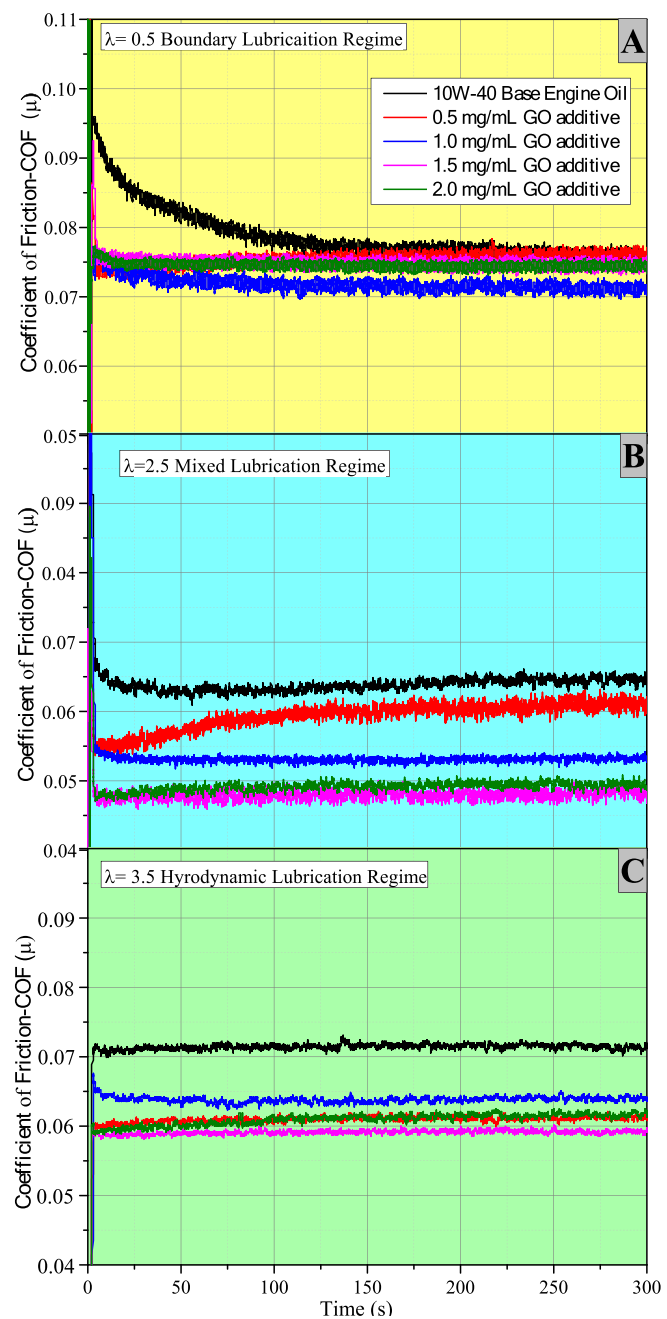


Fig. 9. Examples of friction measurements for boundary, mixed and hydrodynamic lubricating conditions.

Table 3
Changes in COF values under different lubrication regimes.

		SAE 10W-40 Base Engine Oil	0.5 mg/mL GO additive	1.0 mg/mL GO additive	1.5 mg/mL GO additive	2.0 mg/mL GO additive
Boundary Lubrication	Maximum Reduction	–	–12.4 % @ $\lambda = 0.1$	–13.8 % @ $\lambda = 0.1$	–8 % @ $\lambda = 0.1$	–13.16 % @ $\lambda = 0.1$
Mixed Lubrication	Average Value of COF (μ)	0.0822	0.0763	0.0744	0.0742	0.0753
	Maximum Reduction	–	–23.55 % @ $\lambda = 3$	–16.77 % @ $\lambda = 2.5$	–26.147 % @ $\lambda = 3$	–23.04 % @ $\lambda = 2.5$
Hydrodynamic Lubrication	Average Value of COF (μ)	0.0647	0.0586	0.0561	0.05	0.052
	Maximum Reduction	–	–23.56 % @ $\lambda = 3.5$	–13.42 % @ $\lambda = 3.5$	–26.15 % @ $\lambda = 3.5$	–22.5 % @ $\lambda = 3.5$
Average Values for All Lubricating Regimes		0.0664	0.0614	0.0603	0.0539	0.0567
		0.0711	0.0654	0.0636	0.0603	0.0613

friction measurements as an example with 1.5 mg/mL GO nanosheet concentration under conditions of $\lambda = 0.5$ for the boundary lubrication regime (Fig. 9-A), $\lambda = 2.5$ for the mixed lubrication regime (Fig. 9-B) and $\lambda = 3.5$ for the hydrodynamic lubrication regime (Fig. 9-C), where significant reductions in the COFs were obtained. As is also evident from the measurements for 1.5 mg/mL GO nanosheet concentration, the GO nanosheet additive effectively reduced the COF in all lubrication regimes and provided much more efficient lubrication compared to the base engine oil.

The friction reduction and anti-wear effects of GO nanosheets in the base engine oil can be explained by various mechanisms that can occur either alone or in combination, depending on the conditions of the lubrication regime. These mechanisms mainly include interlayer sliding, tribofilm deposition, and repair effects e.g. [14,30,32,36,82]. In the boundary lubrication regime, which occurs under low-speed or high-load conditions, as well as in some conditions in the mixed lubrication regime, friction between the asperities of the contact surfaces is dominant due to the low oil film thickness. In these conditions, the friction is reduced as a result of the easy shearing of the interlayers of multi-layered 2D GO nanosheets caused by the weak Van-der-Waals force [5,30,32,44,54,71,74,86]. Additionally, multi-layered 2D GO nanosheets can be conformally absorbed or deposited on the roughness of the contact surfaces, resulting in the formation of a protective tribo-layer film that prevents direct contact between the surfaces through the third-body effect [15,30,32,36,40,86]. This also covers the concaves and gaps in the roughness of the contact surfaces, providing mending and self-repairing effects. [7,15,30,32,40,86]. The boundary or mixed lubrication regimes mainly develop in internal combustion engines as the piston speed becomes close to zero at the end of the stroke, in the comparatively slow-motion of the valve train components, and during the engine start-up or shutdown phases [8–11,15,17,43]. In these conditions, the interlayer sliding behavior becomes effective with the addition of multi-layered 2D GO nanosheets to the interspaces of the contact points [30,32,45,86]. In the hydrodynamic lubrication regime, which occurs under high-speed or low-load conditions, the hydrodynamic flow of the lubricating oil film completely separates the contact surfaces. Changes in the lubricating oil viscosity with the GO addition become an important factor in the hydrodynamic viscous friction force due to the shearing resistance of the lubricating oil film [4,5]. Multi-layered 2D GO nanosheets, settled between adjacent base engine oil layers, provide relative ease of movement between the base engine oil layers and reduce viscosity as a result of a reduction in shear stress [30,45,69,76,86]. As also mentioned in Section 3.1, the dynamic viscosity values decreased up to 14 % and the VI showed a slight increase of up to 7 % with the addition of multi-layered 2D GO nanosheets at different concentrations when compared with base engine oil. The hydrodynamic lubrication regime develops in internal combustion engines mainly in the crankshaft journal bearings and in some conditions in the piston skirts [8,9,42,43]. Under various engine operating conditions, the oil films tend to shear thinning at high shear rates present in engine components with low engine oil viscosity and high VI [71,76,78]. These reduce friction losses and have a significant effect on mechanical engine efficiency and fuel saving.

The results of WSD measurements performed under boundary and mixed lubrication regimes are given in Fig. 10 and Table 4. As expected, the most wear on the ball specimens was observed under boundary or mixed lubrication regimes with high-load and low-speed conditions. In the hydrodynamic lubrication regime, almost similar results on WSD measurements were observed with GO nanosheet additives due to the mainly viscous lubrication friction. Therefore, the wear results under the hydrodynamic lubrication regime are not given in Fig. 11 and Table 4. However, significantly smaller WSDs were observed at all concentrations of GO nanosheets compared to the base engine oil in both of boundary and mixed lubrication regimes. As shown in Table 4, the results for the boundary lubrication regime showed that the usage of GO nanosheet additives at 0.5, 1, 1.5 and 2.0 mg/mL concentrations

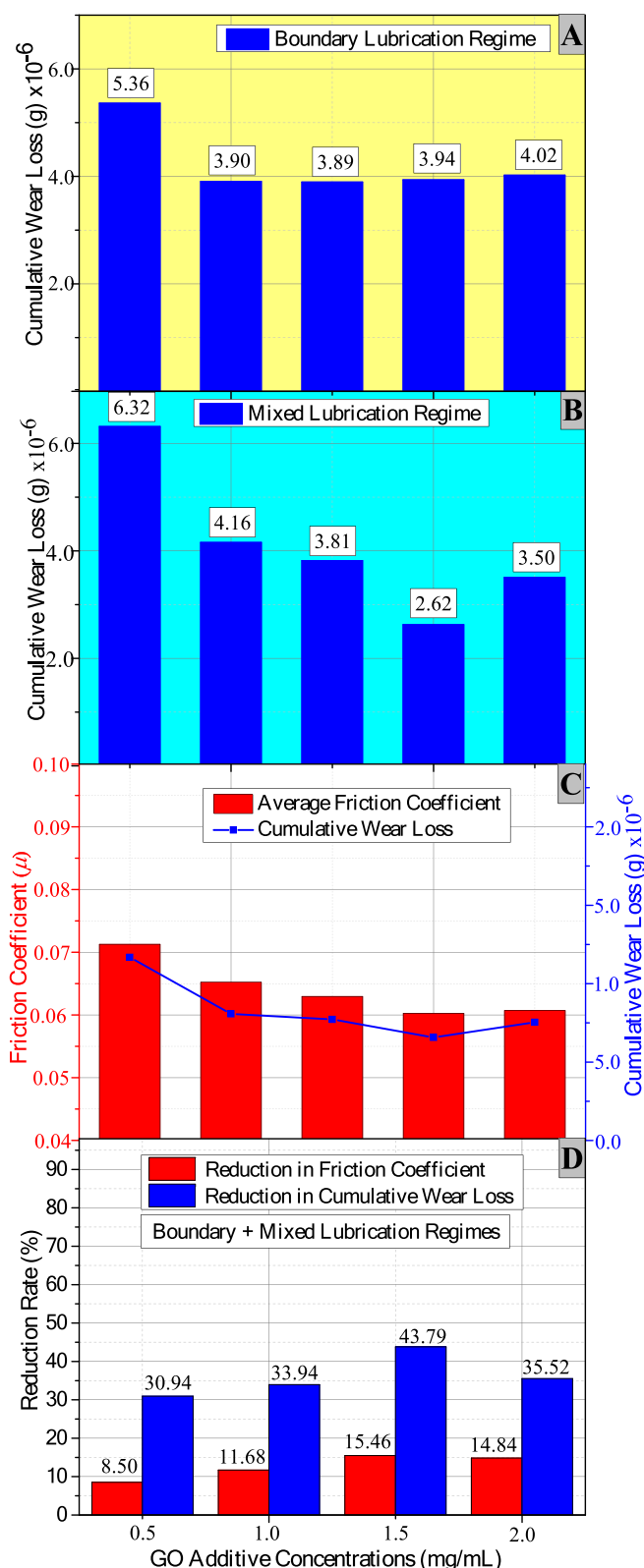


Fig. 10. The effect of GO nanoadditive on the cumulative wear of the ball specimen under boundary and mixed lubricating regimes.

reduced WSDs by up to 14.5 %, 15 %, 24.64 % and 20.26 %, respectively. In the mixed lubrication conditions, the usage of GO nanosheet additives at 0.5, 1, 1.5 and 2.0 mg/mL concentrations reduced WSDs by up to 10.8 %, 19.2 %, 19.3 % and 12.7 %, respectively. Fig. 11 also shows the WSD measurements under conditions of the boundary

Table 4

WSD measurements of the ball specimen under boundary and mixed lubricating regimes.

Stribeck Curve X axis	10 W-40Base Engine Oil	0.5 mg/mL GO additive	1.0 mg/mL GO additive	1.5 mg/mL GO additive	2.0 mg/mL GO additive
0.1	379.28	358.98	346.38	358.41	360.08
0.5	345.28	336.02	332.57	339.65	331.76
0.9	382.73	328.79	345.85	327.95	339.99
1.3	378.92	323.94	322.01	285.54	302.12
1.7	336.86	300.38	297.01	278.26	309.30
2.1	307.17	281.66	274.02	263.38	257.12
2.5	327.51	306.03	264.61	264.30	297.11
3.0	334.13	312.22	324.34	269.64	291.43

lubrication regime at $\lambda = 0.5$ and the mixed lubrication regime at $\lambda = 2.5$, where a significant reduction in the measurements was obtained with 1.5 mg/mL GO nanosheet concentration. Also according to the obtained wear results, the GO nanosheet additive at 1.5 mg/mL concentration was effective in reducing WSD and exhibited good anti-wear resistance. In Fig. 10-A and B, wear mass loss values at each measuring point on the ball specimens are shown cumulatively for both boundary and mixed lubrication regimes. Similar to the COF results, the lowest value in the total wear mass loss was obtained at 1.5 mg/mL GO nanosheet concentration in the mixed lubrication regime. As also seen from Table 4 and Fig. 10-C, the obtained total wear mass loss results are consistent with COF results and have a similar trend for both boundary and mixed lubrication regimes. In Fig. 10-D, the changes in the average COF and total wear mass loss are given as percentages concerning GO nanosheet concentrations for both the boundary and mixed lubrication regimes. Base engine oil containing 1.5 mg/mL GO nanosheet additive showed the best results on tribological performance by reducing the average COF by 17 % and the total wear mass loss by 44 % compared to base engine oil.

Fig. 12 shows SEM images and EDS patterns of the ball specimen's worn surfaces lubricated by base engine oil and base engine oil + 1.5 mg/mL GO nanosheet concentration, under the boundary lubrication

regime at $\lambda = 0.5$. In Fig. 12-A, many wide and deep furrows in the sliding direction, as well as non-uniformly distributed intense pittings are apparent on the worn surface lubricated with base engine oil. In contrast, Fig. 12-B, shows that the furrows and pittings on the worn surfaces are mostly eliminated when lubricated with base engine oil containing 1.5 mg/mL GO nanosheet additive, resulting in a relatively smoother surface compared to the base engine oil lubrication. The EDS patterns in Fig. 12 C and D show that the carbon element on the worn surface lubricated by base engine oil was 8.53 wt%, whereas it was 13.14 wt% on the worn surface lubricated by base engine oil + 1.5 mg/mL GO nanosheet concentration. The difference in carbon element on the worn surfaces was attributed to the C element in the structure of GO nanosheets, indicating the formation of tribo-film as due to the nanoparticles deposition on the worn surface [4,5,54,69,82]. As mentioned earlier, multi-layered 2D GO nanosheets form a protective tribo-layer film on worn surfaces, which provides a smoother and flatter surface with mending and self-repairing effects.

3.4. Engine test results

The engine tests were conducted under steady-state conditions at full load with different speeds ranging from 1700 to 2800 rpm and crankcase oil temperatures between 40 and 100 °C in both firing and motored modes. Since the base engine oil containing 1.5 mg/mL GO nanosheet additive provided the best results in tribological and wear performance tests, the engine tests were performed only using this concentration and compared with the base engine oil results. The engine test results with respect to engine speed at a constant 80 °C engine crankcase oil temperature are shown in Fig. 13. The results indicate that both engine oil samples showed almost similar characteristic trends in all engine performance curves. However, the positive effects of the 1.5 mg/mL GO nanosheet additive are clearly apparent in all engine performance results at each engine speed.

In Fig. 13, it can be observed that the brake torque (M_e) of both lubricant samples reached their maximum value at 2200 rpm due to the improved volumetric efficiency as the engine speed increased. At the maximum M_e point, the intake charge per cycle reaches its maximum

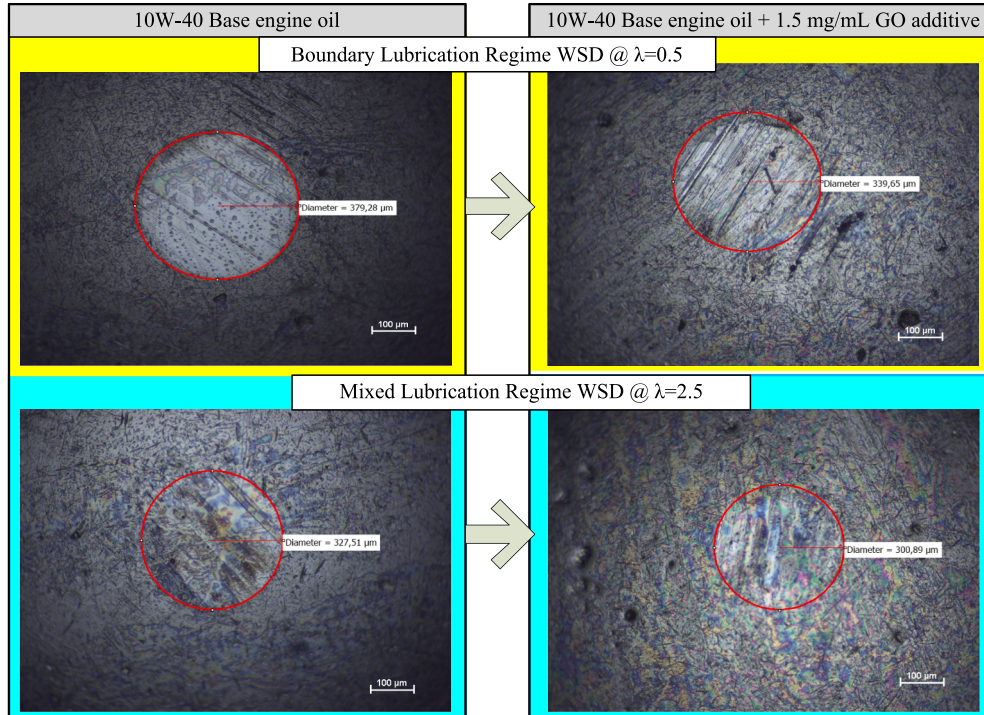


Fig. 11. WSD measurements under conditions of the boundary and mixed lubrication regimes with 1.5 mg/mL GO nanoparticle concentration.

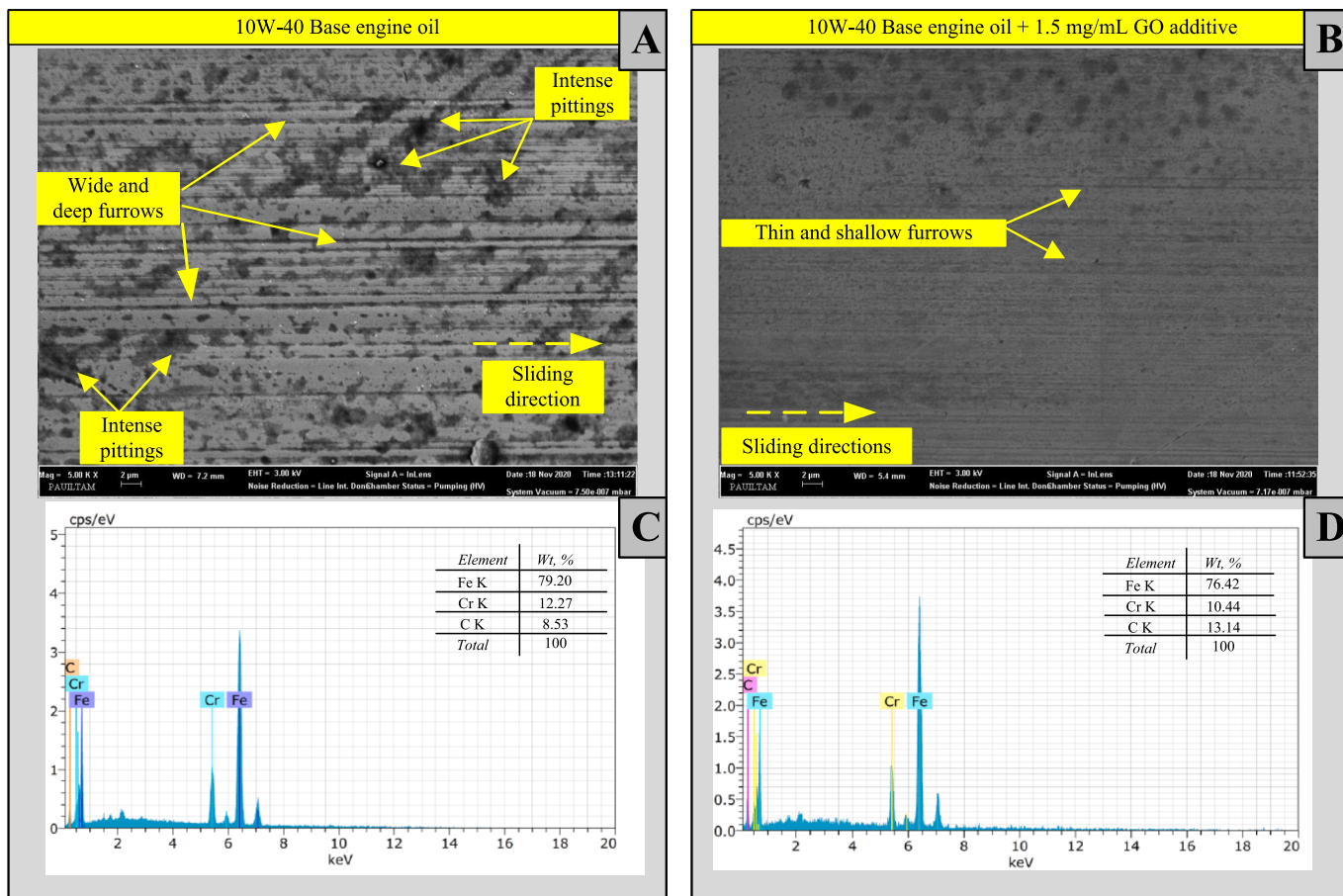


Fig. 12. SEM images and EDS patterns of the ball specimen's worn surfaces under the boundary lubrication regime at $\lambda = 0.5$.

value. After this point, gradual decrements in the M_e occurred mainly due to an increase in frictional losses and a moderate decrease in volumetric efficiency as the engine speed increased [4,5,8,9]. Since P_e is also determined by multiplying the indicated power and the mechanical efficiency, even though the indicated power continues to increase with increasing engine speed, P_e reaches its maximum value at some point. [8,9,87]. As shown in Fig. 13, the P_e of both lubricant samples tends to increase continuously as the engine speed increases up to 2800 rpm. However, if the engine speed continued to increase until the maximum engine speed of 3600 rpm, it is expected that the P_e would reach its maximum value despite decreasing M_e due to increasing cyclic frequency. In the case of a further increase in engine speed, the effect of a decrease in mechanical efficiency would also dominantly lead to a decrease in P_e [9]. However, the GO nanosheet additive resulted in 4.9 % higher M_e at the maximum torque speed of 2200 rpm, and 2.9 % higher P_e at 2800 rpm. Based on the average of five engine speeds, both M_e and P_e were almost 1.1 % higher with the GO nanosheet additive.

In Fig. 13, it can be observed that the $bsfc$ of both lubricant samples decreased with engine speed until reaching a minimum value at around 2200 rpm, after this point increased again with increasing engine speed. Conversely, the thermal efficiency (η_t) of both lubricant samples showed an opposite trend to $bsfc$ with increases in engine speed. This is mainly because the heat losses decrease and combustion efficiency improves with increasing engine speed up to the point of a minimum value of $bsfc$ and a maximum value of bte [4,5,8,9,87]. On the other hand, at higher engine speeds, the frictional losses become more significant as engine frictional power increases almost proportionally to the square of the engine speed [9]. Also, with the use of GO nanosheet additive, a reduction of up to 5.69 % in $bsfc$ and an improvement of up to 6 % in bte were observed at 2200 rpm. Based on the average of five engine speeds,

$bsfc$ decreased by %2.6 and bte was 2.7 % higher with the GO nanosheet additive.

Fig. 13 also shows that motored torque (M_m) of both lubricant samples, which represents the total engine frictional losses, increased linearly with the increase in engine speed [5,8,9,68]. Therefore, the engine frictional power (P_f) would show an increase approximately proportional to the square of the engine speed. Conversely, the mechanical efficiency (η_m) of both lubricant samples decreased almost linearly with the increase in engine speed. However, the addition of GO nanosheet additives resulted in up to a 6 % reduction in the motored torque and up to a 2.4 % improvement in the mechanical efficiency (η_m) at 2800 rpm. These results suggest that using GO nanosheet additives to reduce engine frictional losses also offers significant potential to save fuel consumption and thus reduce CO₂ emissions. Because, the difference between the lowest and highest points in the results obtained means a reduction in fuel consumption, CO₂ emissions, and an increase in P_e . However, although motored engine test results give a better overview of lubricants' performance, they lack specific tribological insights on the component base of engines since they operate under different tribological regimes. As explained in Section 3.3, depending on the lubrication regime conditions, the friction reduction and anti-wear effects of GO nanosheets in the base engine oil are explained by various mechanisms that can occur alone or in combination, such as interlayer sliding, tribofilm deposition and repair effects [14,15,30,32,36,37]. In this regard, when the engine speed increases, the hydrodynamic (viscous) friction for both lubricant samples gradually increases with the increase in sliding speed at the friction surfaces between the majority of individual engine parts. As a result, motored torque increases and mechanical efficiency decreases with an increase in the engine speed. In mixed or hydrodynamic lubrication, changes in

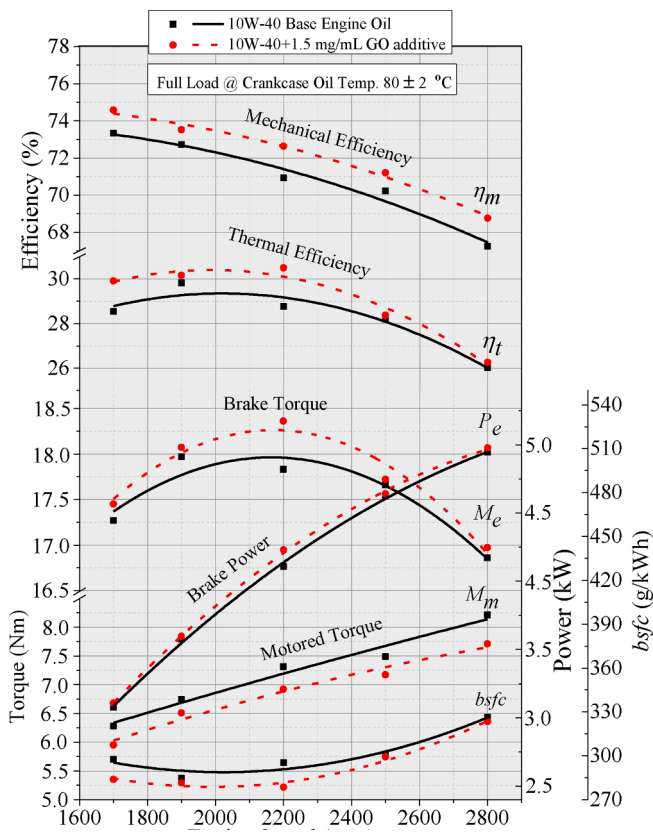


Fig. 13. Engine performance results with respect to engine speed at 80 °C crankcase oil temperature.

lubricant viscosity at the operating temperature and shear rate at different engine speeds are dominant factors [4]. Under these conditions, Adding GO nanosheet additives to the lubricant can improve the viscosity-temperature-shear rate characteristics, leading to friction reduction achieved with low viscosity and high VI [28,29,76]. Fig. 14A-B-C also shows the variation of frictional power (P_f) for both lubricant samples at constant engine speeds of 1700, 2200 and 2800 rpm with respect to engine crankcase oil temperatures. The frictional power decreases in both oil samples with an increase in engine oil temperature at three different engine speeds. However, frictional power was significantly reduced with the GO nanosheets additive at each engine speed and oil temperature, and this reduction was around 3.7 % on average. In Fig. 14-D shows that engine oil with GO nanosheet additives provides the most effective friction reduction performance compared to the base engine oil when the engine oil temperature was around 80–90 °C. When the oil temperature is raised to 100 °C and above, the tendency to decrease in friction power slows down due to deviations from optimum viscosity values. An optimum viscosity that provides minimum engine friction exists at a given engine speed and load because the engine has both hydrodynamic and mixed/boundary lubrication components.

4. Conclusions

In this study, a fully synthetic SAE 10W-40 engine oil was used as the base engine oil, and GO nanosheets were added to the base engine oil in 4 different proportions (0.5, 1.0, 1.5, 2.0 mg/mL). The dynamic viscosity values decreased by up to 5 %, especially at temperatures above 40 °C. The VI of the samples slightly increased by up to 7 % with the addition of GO nanosheets additives at different concentrations compared to the base engine oil. The thermal conductivity of the base engine oil increased in the range of 4–15 % with GO nanosheet additives at all concentrations.

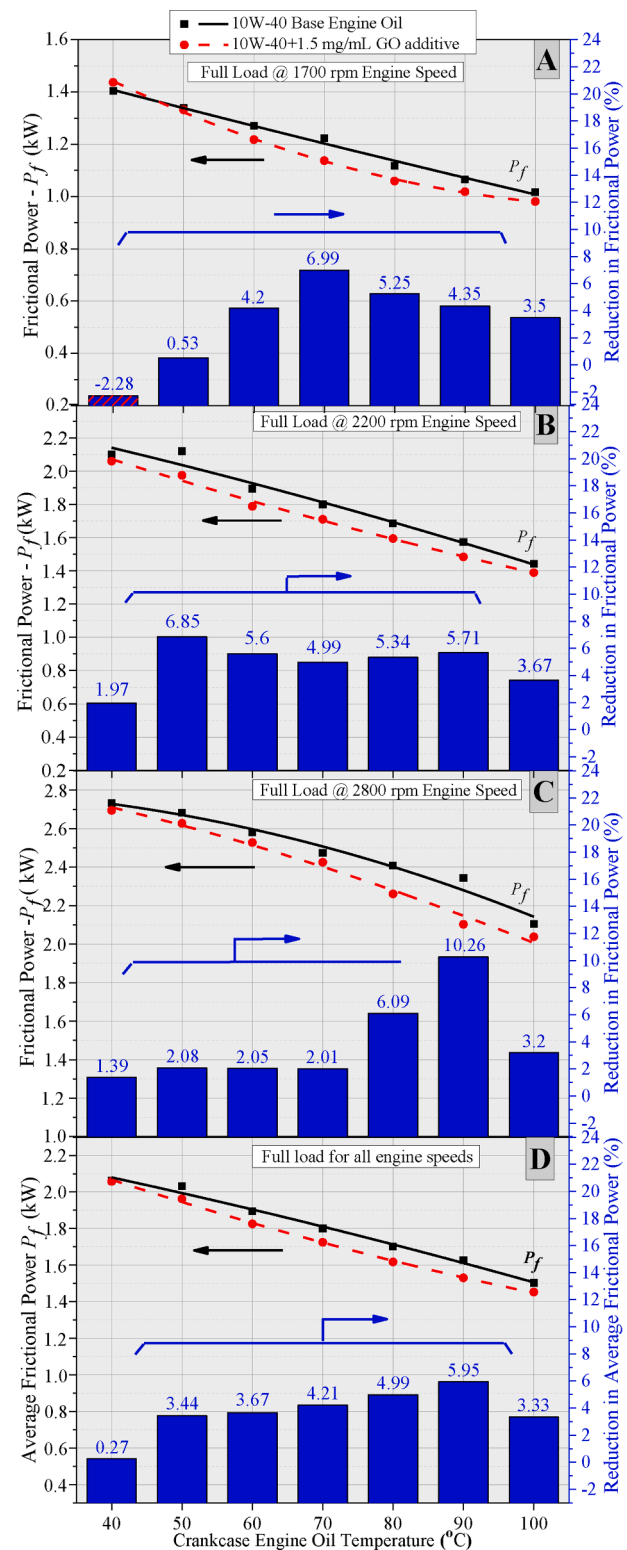


Fig. 14. Engine frictional power results with respect to different crankcase oil temperatures.

4.1. In the tribological test results

The additions of GO nanosheets caused significantly lower COFs and smaller WSDs in all lubrication regimes. GO nanosheets at 1.0 mg/mL and 1.5 mg/mL concentrations resulted in reductions of up to 13.8 % and 26 % in COF, respectively. Although the COFs slightly increased in

all lubrication regimes when the concentration was increased to 2.0 mg/mL compared to 1.5 mg/mL, they remained below the values of the base engine oil. The total wear mass loss results for both the boundary and mixed lubrication regimes were consistent with the COF results and exhibited a similar trend. The best GO concentration amount was determined as 1.5 mg/mL with its tribological performance in the mixed lubrication regime.

4.2. In the engine test results

The addition of GO nanosheet additive at a concentration of 1.5 mg/mL resulted in a reduction up to 6 % in the motored torque, which represents engine frictional losses. An improvement up to 2.4 % in the mechanical efficiency (η_m) at 2800 rpm engine speed were observed. Frictional power was significantly reduced with the GO nanosheet additive at each engine speed and different oil temperature, with an average reduction of around 3.7 %. The M_e was 4.9 % higher at the maximum torque speed of 2200 rpm, and the P_e was 2.9 % higher at 2800 rpm with the use of the GO nanosheets additive. Based on the average of five engine speeds, both M_e and P_e were almost 1.1 % higher. A reduction of up to 5.69 % in $bsfc$ and an improvement of up to 6 % in bte were observed at 2200 rpm with the GO nanosheets additive. Based on the average of five engine speeds, $bsfc$ decreased by %2.6 and bte was 2.7 % higher.

The results of this study demonstrate that the GO nanosheets additives for engine lubricating oils have great potential to exhibit several roles, including viscosity modifier, anti-friction, and anti-wear properties. These properties can enhance the mechanical efficiency of internal combustion engines in the transportation sector, leading to energy and fuel savings, and indirectly contributing to reducing CO₂ emissions. However, detailed and long-term studies are needed on the effects of this additive on the engine warm-up phase, engine durability and service life and sustainability of existing commercial engine oils.

Declaration of Competing Interest

The authors declare that they have no known competing financial interests or personal relationships that could have appeared to influence the work reported in this paper.

Acknowledgment

This research was conducted as part of the 2019FEBE035 project funded by the Pamukkale University Scientific Research Council, in association with the master thesis of Özgür Çetin. Therefore, the authors would like to thank Pamukkale University. Additionally, the authors are also very grateful to Assoc. Prof. Dr. Erkan ÖZTÜRK for his assistance; Prof. Dr. Cem GÖK for the preparation of additives with oleic acid; Assoc. Prof. Dr. İsmail OVALI for allowing use of the pin-on-disc tribometer; Prof. Dr. Nazim USTA for conducting viscosity measurements; Prof. Dr. Sami Gökhan ÖZKAL for providing access to the thermal conductivity test apparatus; Prof. Dr. Numan B. BEKTAS and Res. Asst. İnan AĞIR for allowing use of the ultrasonic mixer device.

References

- [1] K. Holmberg, P. Andersson, A. Erdemir, Global energy consumption due to friction in passenger cars, *Tribol. Int.* 47 (2012) 221–234.
- [2] K. Holmberg, P. Andersson, N.O. Nylund, K. Mäkelä, A. Erdemir, Global energy consumption due to friction in trucks and buses, *Tribol. Int.* 78 (2014) 94–114.
- [3] K. Holmberg, A. Erdemir, The impact of tribology on energy use and CO₂ emission globally and in combustion engine and electric cars, *Tribol. Int.* 135 (2019) 389–396.
- [4] M.K.A. Ali, P. Fuming, H.A. Younus, M.A.A. Abdelkareem, F.A. Essa, A. Elagouz, H. Xianjun, Fuel economy in gasoline engines using Al₂O₃/TiO₂ nanomaterials as nanolubricant additives, *Appl. Energy* 211 (2018) 461–478.
- [5] M.K.A. Ali, H. Xianjun, M.A.A. Abdelkareem, M. Gulzar, A.H. Elsheikh, Novel approach of the graphene nanolubricant for energy saving via antifriction/wear in automobile engines, *Tribol. Int.* 124 (2018) 209–229.
- [6] J.P. Singh, S. Singh, T. Nandi, S.K. Ghosh, Development of graphitic lubricant nanoparticles based nanolubricant for automotive applications: Thermophysical and tribological properties followed by IC engine performance, *Powder Technol.* 387 (2021) 31–47.
- [7] S.J. Hettiarachchi, J. Bowen, M. Kershaw, I.A. Baragau, A. Nicolaev, S. Kellici, Nanostructured Al₂O₃/graphene additive in bio-based lubricant: A novel approach to improve engine performance, *Tribol. Int.* 186 (2023), 108619.
- [8] Pulkabek W.W., Engineering Fundamentals of the Internal Combustion Engine, Pearson Prentice Hall, Upper Saddle River, N.J., pages: 50-52, 56, 57, 349-359, 368-369, 2004.
- [9] Ferguson C. R., Kirkpatrick A., Internal Combustion Engines: Applied Thermosciences, Thirt Edition, John Wiley & Sons, Inc., Chichester, West Sussex, United Kingdom, Pages: 288, 312-315, 372,373, 2016.
- [10] R.I. Taylor, R.C. Coy, Improved Fuel Efficiency by Lubricant Design: a Review, *Proceedings of the Institution of Mechanical Engineers, Part J: Journal of Engineering Tribology* 214 (1) (2000) 1–15.
- [11] R.I. Taylor, R. Mainwaring, R.M. Mortier, Engine Lubricant Trends Since 1990, *Proceedings of the Institution of Mechanical Engineers, Part J: Journal of Engineering Tribology* 219 (5) (2005) 331–346.
- [12] Haycock R.F., Hillier J.E., Automotive Lubricants Reference Book, Second Edition, SAE International, Warrendale, Pa. 3-5, 63-85, 2004.
- [13] S.R. Kadhim, H.J. Kadhim, A.K. Shakir, Investigation of tribological properties of oleic acid-modified RGO-based engine oil nano fluid, *NeuroQuantology* 18 (6) (2020) 49–54.
- [14] M. Gulzar, H.H. Masjuki, M.A. Kalam, M. Varman, N.W.M. Zulkifli, R.A. Mufti, R. Zahid, Tribological performance of nanoparticles as lubricating oil additives, *J. Nanopart. Res.* 18 (8) (2016) 223.
- [15] A.K. Rasheed, M. Khalid, W. Rashmi, T.C.S.M. Gupta, A. Chan, Graphene based nanofluids and nanolubricants - review of recent developments, *Renew. Sustain. Energy Rev.* 63 (2016) 346–362.
- [16] H. Rahnejat, Tribology and Dynamics od Engine and Powertrain, Fundamentals, Applications and Future Trends, Woodhead Publishing Limited, Philadelphia, PA, 2010, pp. 254–255.
- [17] N.D.S.A. Santos, V.R. Roso, M.T.C. Faria, Review of engine journal bearing tribology in start-stop applications, *Eng. Fail. Anal.* 108 (2020), 104344.
- [18] H. Shao, J.W. Roos, J.E. Remias, Evaluation of the role of lubricant additives in emission control, *Lubricants* 10 (12) (2022), 362.
- [19] M.F. Sgroi, M. Asti, F. Gilli, F.A. Deorsola, S. Bensaid, D. Fino, G. Kraft, I. Garcia, F. Dassenoy, Engine bench and road testing of an engine oil containing MoS₂ particles as nano-additive for friction reduction, *Tribol. Int.* 105 (2017) 317–325.
- [20] S.V. Sanchez, G.D. Yadav, Synthesis of environment-friendly, sustainable, and nonotoxic bio-lubricants: a critical review of advances and a path forward, *Biofuels Bioproducts and Biorefining-BIOFPR* 16 (5) (2022) 1172–1195.
- [21] M.K.A. Ali, H. Xianjun, Improving the tribological behavior of internal combustion engines via the addition of nanoparticles to engine oils, *Nanotechnol. Rev.* 4 (4) (2015) 347–358.
- [22] Fenske G., Ajayi L., Demas N., Erck R., Lorenzo-Martin C., Erdemir A., and Eryilmaz O., Engine Friction Reduction Technologies, Argonne National Laboratory, Project ID # FT012, presentation, 2014.
- [23] A. Young, Fuel economy drives change for passenger car oil formulations, *Lube Magazine* 128 (2015) 25–28.
- [24] S. Yulia, Improving fuel efficiency by selecting the right oil, *Tribology and Lubrication Technology* 79 (1) (2023) 32–37.
- [25] J. Zhao, Y. Huang, Y. He, Y. Shi, Nanolubricant additives: a review, *Friction* 9 (5) (2021) 891–917.
- [26] M. Hatami, M. Hasanzadeh, D. Jing, Recent developments of nanoparticles additives to the consumables liquids in internal combustion engines: Part II: nano-lubricants, *J. Mol. Liq.* 319: Article Number: 114156 (2020).
- [27] Mo, Y., Wang, J., Hong, Y., Yang, X. et al., Study on the Influence of Low-Viscosity Engine Oil on Engine Friction and Vehicle Worldwide Harmonized Light Vehicles Test Cycle Fuel Economy, SAE Technical Paper No: 2020-01-5062, 2020.
- [28] Permude A., Pathak M., Kumar V., Singh S., Influence of Low Viscosity Lubricating Oils on Fuel Economy and Durability of Passenger Car Diesel Engine, SAE Technical Paper No: 2012-28-0010, 2012.
- [29] Okuyama Y., Shimokoji D., Sakurai T., and Maruyama M., Study of Low-Viscosity Engine Oil on Fuel Economy and Engine Reliability, SAE Technical Paper No: 2011-01-1247, 2011.
- [30] H. Xiao, S. Liu, 2D nanomaterials as lubricant additive: a review, *Mater. Des.* 135 (2017) 319–332.
- [31] W. Liu, X. Qiao, S. Liu, P. Chen, A review of nanomaterials with different dimensions as lubricant additives, *Nanomaterials* 12 (21) (2022), 3780.
- [32] Q. Gao, S. Liu, K. Hou, Z. Li, J. Wang, Graphene-based nanomaterials as lubricant additives: a review, *Lubricants* 10 (10) (2022), 273.
- [33] M. Waqas, R. Zahid, M.U. Bhutta, Z.A. Khan, A. Saeed, A review of friction performance of lubricants with nano additives, *Materials* 14 (21) (2021), 6310.
- [34] B. Wang, F. Qiu, G.C. Barber, Q. Zou, J. Wang, S. Guo, Y. Yuan, Q. Jiang, Role of nano-sized materials as lubricant additives in friction and wear reduction: a review, *Wear* 490–491 (2022), 204206.
- [35] S. Shahnaz, S. Bagheri, S.B.A. Hamid, Enhancing lubricant properties by nanoparticle additives, *Int. J. Hydrogen Energy* 41 (4) (2016) 3153–3170.
- [36] Y. Guo, X. Zhou, K. Lee, C.H. Yoon, Q. Xu, D. Wang, Recent development in friction of 2D materials: from mechanisms to applications, *Nanotechnology* 32 (31) (2021), 312002.
- [37] J. Zhao, T. Gao, Y. Li, Y. He, Y. Shi, Two-dimensional (2D) graphene nanosheets as advanced lubricant additives: a critical review and prospect, *Materials Today Communications* 29 (2021), 102755.

- [38] A. Koita, S. Borkakoti, S.K. Ghosh, Wear and performance analysis of a 4-stroke diesel engine employing nanolubricants, *Particuology* 37 (2018) 54–63.
- [39] P.K. Sarma, V. Srinivas, V.D. Rao, A.K. Kumar, Experimental study and analysis of lubricants dispersed with nano Cu and TiO₂ in a four-stroke two wheeler, *Nanoscale Research Letters* 6 (2011), 233.
- [40] G. Singh, M.F. Wani, M.M. Wani, An experimental study on fuel energy saving in gasoline engines using GNP as a lubricant additive, *International Journal of Engine Research* 23 (12) (2021) 2184–12144.
- [41] Y.F. Lu, W.L. Hsiao, Y.S. Chen, Tribology performance of silica nanoparticles as lubricant additives in a reciprocating four-stroke engine motorcycle, *Int. J. Automot. Technol.* 24 (2) (2023) 435–444.
- [42] R.I. Taylor, N. Morgan, R. Mainwaring, T. Davenport, How much mixed/boundary friction is there in an engine - and where is it? Proceedings of the Institution of Mechanical Engineers, Part J: Journal of Engineering Tribology 234 (10) (2019) 1563–1579.
- [43] C.M. Taylor, Lubrication regimes and the internal combustion engine, *Tribology Series* 26 (1993) 75–87.
- [44] A. Senatore, V. D'Agostino, V. Petrone, P. Ciambelli, M. Sarno, Graphene oxide nanosheets as effective friction modifier for oil lubricant: materials, methods, and tribological results, *ISRN Tribology* (2013). Article Number: 425809, 2013.
- [45] B. Gupta, N. Kumar, K. Panda, S. Dash, A.K. Tyagi, Energy Efficient Reduced Graphene Oxide Additives: Mechanism of Effective Lubrication and Antiwear Properties, *Sci. Rep.* 6 (2016), 18372.
- [46] M.M. Rahman, M. Islam, R. Roy, H. Younis, M. AlNahyan, H. Younes, Carbon nanomaterial-based lubricants: review of recent developments, *Lubricants* 10 (11) (2022), 281.
- [47] L. Liu, M. Zhou, L. Jin, L. Li, Y. Mo, G. Su, X. Li, H. Zhu, Y. Tian, Recent advances in friction and lubrication of graphene and other 2D materials: Mechanisms and applications, *Friction* 7 (3) (2019) 199–216.
- [48] H.A. Zaharin, M.J. Ghazali, N. Thachatharen, F. Ezzah, R. Walvekar, M. Khalid, Progress in 2D materials based nanolubricants: a review, *FlatChem* 38 (2023), 100485.
- [49] Cao N. and Zhang Y., Study of Reduced Graphene Oxide Preparation by Hummers' Method and Related Characterization, *Journal of Nanomaterials*, 2015: Article Number: 168125, 2015.
- [50] B. Paulchamy, G. Arthi, B.D. Lignesh, A simple approach to stepwise synthesis of graphene oxide nanomaterial, *Journal of Nanomedicine & Nanotechnology* 6 (1) (2015), 1000253.
- [51] K. Krishnamoorthy, M. Veerapandian, K. Yun, S.-J. Kim, The chemical and structural analysis of graphene oxide with different degrees of oxidation, *Carbon* 53 (2013) 38–49.
- [52] G.K. Yogesh, E.P. Shuaib, P. Roopmani, M.B. Gumpu, U.M. Krishnan, D. Sastikumar, Synthesis, characterization and bioimaging application of laser-ablated graphene-oxide nanoparticles (nGOs), *Diam. Relat. Mater.* 104 (2020), 107733.
- [53] W. Zhang, M. Zhou, H. Zhu, Y. Tian, K. Wang, J. Wei, F. Ji, X. Li, Z. Li, P. Zhang, D. Wu, Tribological properties of oleic acid-modified graphene as lubricant oil additives, *Journal of Physics D: Applied Physics* 44 (22) (2011), 205303.
- [54] J. Lin, L. Wang, G. Chen, Modification of graphene platelets and their tribological properties as a lubricant additive, *Tribol. Lett.* 41 (1) (2011) 209–215.
- [55] T. Chen, Y. Xia, Z. Jia, Z. Liu, H. Zhang, Synthesis, characterization, and tribological behavior of oleic acid capped graphene oxide, *Journal of Nanomaterials* (2014), 654145.
- [56] Anonymous, ASTM, D2270-04, Standard Practice for Calculating Viscosity Index from Kinematic Viscosity at 40 and 100, 1-6, (2007).
- [57] Anonymous, Thermal Conductivity of Liquids and Gases Unit, Series H470. Experimental Operating and Maintenance Manual, P.A. Hilton Ltd., England, 1994.
- [58] S.G. Özkal, Y. Tülek, Experimental determination of thermal conductivity of various milk and vegetable oil products, *Turk. J. Eng. Environ. Sci.* 25 (1) (2001) 51–60.
- [59] M. Al-Amayreh, Experimental study of thermal conductivity of ethylene glycol water mixtures, *Journal of Engineering Research and Application* 10 (1) (2020) 62–68.
- [60] Y.R. Sekhar, K.V. Sharma, M.T. Naik, L.S. Sundar, Experimental investigations on thermal conductivity of water and Al₂O₃ nanofluids at low concentrations, *International Journal of Nanoparticles* 5 (4) (2012) 300–315.
- [61] Anonymous, ASTM, G99-95a, Standard Test Method for Wear Testing with a Pin-on-Disk Apparatus, 1-6, 2000.
- [62] M.K.A. Ali, H. Xianjun, L. Mai, C. Qingping, R.F. Turkson, C. Bicheng, Improving the tribological characteristics of piston ring assembly in automotive engines using Al₂O₃ and TiO₂ nanomaterials as nanolubricant additives, *Tribol. Int.* 103 (2016) 540–554.
- [63] H. Yu, Y. Xu, P. Shi, W. Hongmei, M. Wei, K. Zhao, B. Xu, Microstructure mechanical properties and tribological behavior of tribofilm generated from natural serpentine mineral powders as lubricant additive, *Wear* 297 (2013) 802–810.
- [64] V. Zin, F. Agresti, S. Barison, L. Colla, E. Mercadelli, M. Fabrizio, C. Pagura, Tribological properties of engine oil with carbon nano-horns as nano-additives, *Tribol. Lett.* 55 (1) (2014) 45–53.
- [65] N. Noorawzi, S. Samion, Tribological effects of vegetable oil as alternative lubricant: a pin-on-disk tribometer and wear study, *Tribol. Trans.* 59 (5) (2016) 831–837.
- [66] S.J. Harris, G.G. Krauss, Improved technique for measuring the ball volume removed in a ball-on-disk test, *Tribol. Lett.* 10 (3) (2001) 187–188.
- [67] X. Li, M. Sosa, U. Olofsson, A pin-on-disc study of the tribology characteristics of sintered versus standard steel gear materials, *Wear* 340 (2015) 31–40.
- [68] Yagi S. and Ishibasi Y., Sono H., Experimental Analysis of Total Engine Friction in Four Stroke S. I. Engines, SAE technical papers, Paper No: 900223, 1990.
- [69] Y.B. Guo, S.W. Zhang, The tribological properties of multi-layered graphene as additives of PAO₂ oil in steel-steel contacts, *Lubricants* 4 (3) (2016) 2–12.
- [70] K. Apmann, R. Fulmer, A. Soto, S. Vafaei, Thermal conductivity and viscosity: review and optimization of effects of nanoparticles, *Materials* 14 (5) (2021), 1291.
- [71] K.K. Mishra, K. Panda, N. Kumar, D. Malpani, T.R. Ravindran, P. Khatri Om, Nanofluid lubrication and high pressure Raman studies of oxygen functionalized graphene nanosheets, *Chemistry* 61 (2018) 97–105.
- [72] E.O.B Ettefaghi, H. Ahmadi, A. Rashidi, A. Nouralishahi, S.S. Mohtasebi, Preparation and thermal properties of oil-based nanofluid from multi-walled carbon nanotubes and engine oil as nano-lubricant, *Int. Commun. Heat Mass Transfer* 46 (2013) 142–147.
- [73] R. Ranjbarzadeh, R. Chaabane, Experimental study of thermal properties and dynamic viscosity of graphene oxide/oil nano-lubricant, *Energies* 14 (10) (2021), 2886.
- [74] J. Patel, G. Pereira, D. Irvine, A. Kiani, Friction and wear properties of base oil enhanced by different forms of reduced graphene friction and wear properties of base oil enhanced by different forms of reduced graphene, *AIP Advances* 9 (4) (2019), 045011.
- [75] B. Alqahtani, W. Hoziefa, H.M. Abdel Moneam, M. Hamoud, S. Salunkhe, A. B. Elshalakany, M. Abdel-Mottaleb, J.P. Davim, Tribological performance and rheological properties of engine oil with graphene nano-additives, *Lubricants* 10 (7) (2022), 137.
- [76] N. Marx, L. Fernández, F. Barceló, H. Spikes, Shear thinning and hydrodynamic friction of viscosity modifier-containing oils. Part I: shear thinning behavior, *Tribol. Lett.* 66 (3) (2018), 92.
- [77] R.A. Mufti, M. Priest, Effect of engine operating conditions and lubricant rheology on the distribution of losses in an internal combustion engine, *Journal of Tribology* 131 (4) (2009), 041101.
- [78] A. Martini, U.S. Ramasamy, M. Len, Review of Viscosity Modifier Lubricant Additives, *Tribology Letters* 66 (2) (2018), 58.
- [79] M.K.A. Ali, H. Xianjun, R.F. Turkson, Z. Peng, X. Chen, Enhancing the thermophysical properties and tribological behaviour of engine oils using nanolubricant additives, *RCS Advances* 6 (81) (2016) 77913–77924.
- [80] M. Muthuraj, J.B. Raj, J. Suni, Experimental investigation on the inuence of graphene nanoplatelets dispersion on the thermal conductivity of sun flower oil, *International Journal of Nanoscience* 19 (2) (2019), 1950011.
- [81] P. Dhar, S.S. Gupta, S. Chakraborty, A. Pattamatta, K.D. Sarit, The role of percolation and sheet dynamics during heat conduction in poly-dispersed graphene nanofluids, *Applied Physics Letters* 102 (16) (2013), 163114.
- [82] A.K. Rasheed, M. Khalid, A. Javeed, W. Rashmi, T.C.S.M. Gupta, A. Chan, Heat transfer and tribological performance of graphene nanolubricant in an internal combustion engine, *Tribol. Int.* 103 (2016) 504–515.
- [83] S. Daviran, A. Kasaeian, H. Tahmooressi, A. Rashidi, D. Wen, O. Mahian, Evaluation of clustering role versus Brownian motion effect on the heat conduction in nanofluids: a novel approach, *Int. J. Heat Mass Transf.* 108 (2017) 822–829.
- [84] M. Kole, T.K. Dey, Role of interfacial layer and clustering on the effective thermal conductivity of CuO–gear oil nanofluids, *Experimental Thermal Fluid Science*. 35 (7) (2011) 1490–1495.
- [85] N.R. Karthikeyan, J. Philip, B. Raj, Effect of clustering on the thermal conductivity of nanofluids, *Mater. Chem. Phys.* 109 (1) (2008) 50–55.
- [86] N. Nyholm, N. Espallargas, Functionalized carbon nanostructures as lubricant additives – a review, *Carbon* 201 (2023) 1200–1228.
- [87] Heywood J. B., Internal Combustion Engine Fundamentals 2E, McGraw-Hill Education, New York, N.Y., Pages: 1379-1384, 1192-1209, 2019.